THE ASTROPHYSICAL JOURNAL, 369:L67–L70, 1991 March 10

FIRST RESULTS FROM THE FAINT OBJECT CAMERA: IMAGING THE CORE OF R AQUARII[1]

F. PARESCE,[2,3,4] R. ALBRECHT,[2,4,5] C. BARBIERI,[2,6] J. C. BLADES,[2,3,5] A. BOKSENBERG,[2,7] P. CRANE,[2,8]
J. M. DEHARVENG,[2,9] M. J. DISNEY,[2,10] P. JAKOBSEN,[2,11] T. M. KAMPERMAN,[2,12] I. R. KING,[2,13]
F. MACCHETTO,[2,3,4] C. D. MACKAY,[2,14] G. WEIGELT,[2,15] D. BAXTER,[3] P. GREENFIELD,[3]
R. JEDRZEJEWSKI,[3] A. NOTA,[3,16] AND W. B. SPARKS[3]

Received 1990 October 15; accepted 1990 November 20

ABSTRACT

The Faint Object Camera on the *Hubble Space Telescope* was used to observe the inner regions of the symbiotic Mira variable R Aquarii through two filters centered on the [O III] 5007 Å and the [O II] 3727 Å nebular emission lines. Both images show bright arcs, knots, and filaments superposed on fainter, diffuse nebulosity extending in a general SW–NE direction from the Mira variable to the edge of the field at 10″ distance. The observed nebulosity is brighter and more complex in its northern extension where it attains a surface brightness of order 10^{-12} ergs cm^{-2} s^{-1} arcsec^{-2} in the [O III] line. Although saturated due to the strong signal, the core is resolved in both lines into at least two bright knots of emission whose positions and structure are aligned with PA = 50°. The central knots appear to be the source of a continuous, well-collimated, stream of material extending out to 3″–4″ in the northern sector corresponding to a linear distance of approximately 1000 AU. The northern stream seems to bend around an opaque obstacle and form a spiral before breaking up into discrete wisps and knots deviating toward the north. The southern stream is composed of smaller, discrete parcels of emitting gas curving to the SE. A preliminary estimate of the [O III]–to–[O II] line ratio in the filaments shows that it is significantly higher than 1 indicating either that the features are density-bounded or that the ionizing radiation field has a nonthermal power-law form.

Subject headings: nebulae: individual (R Aqr) — stars: individual (R Aqr) — stars: symbiotic

1. INTRODUCTION

R Aquarii is a long-period M7e Mira variable and a dusty type symbiotic at a distance of about 250 pc (Kenyon 1986). It oscillates between $V = 6$ and 12 mag, approximately, with a 387 day period, but disruptions of the light curve have been well documented (Mattei & Allen 1979). The most recent disturbance occurred in the 1922–1933 time frame when the star ceased to vary significantly and the spectrum turned blue with prominent P Cygni–type emission lines (Merrill 1950). R Aqr is a prominent source at all wavelengths from the soft X-ray to the radio region (see Whitelock 1987; Schulte-Ladbeck 1988; Michalitsianos & Kafatos 1988 for recent reviews). The source is surrounded by arcminute-sized arcs of nebulosity expanding at several tens of km s^{-1} with about 5×10^{42} ergs of kinetic energy, most probably due to recurring nova-like eruptions (Solf & Ulrich 1985). In the past decade, a bright jet in the inner core has appeared and has been observed to vary in structure and/or brightness on short time scales (Paresce, Burrows, & Horne 1988; Burgarella & Paresce 1991).

The origin of the jet and the outer nebulosity is still controversial and unresolved by presently available measurements. Our understanding is severely hampered by the sporadic coverage of a complex, time-varying phenomenon and the lack of spatial resolution and discrimination against the glare of the bright Mira variable and surrounding compact nebulosity. A number of mechanisms for their formation and development have been proposed (see discussion in Paresce et al. 1988 and Willson 1988), but the source or sources of the bewildering array of phenomena in this star has remained shrouded in mystery. It is not clear whether R Aquarii is a typical example of a symbiotic that we fortuitously see very close up or that it is a unique type of object.

In an effort to better understand R Aqr and place it in the proper astronomical context, the Faint Object Camera (FOC) on the *Hubble Space Telescope* (*HST*) was pointed toward the core of R Aquarii for a few exploratory images. This *Letter* describes the preliminary results obtained from this investigation in the form of the first very high resolution images of the inner core of R Aqr mainly in the ionized oxygen emission lines in the optical. A subsequent publication will discuss the results, the comparison with ground-based data, and the theoretical implications in greater detail.

[1] Based on observations with the NASA/ESA *Hubble Space Telescope*, obtained at the Space Telescope Science Institute, which is operated by AURA, Inc., under NASA contract NAS 5-26555.

[2] Member FOC Investigation Definition Team.
[3] Postal address: Space Telescope Science Institute, 3700 San Martin Drive, Baltimore, MD 21218.
[4] Astrophysics Division, Space Science Department of ESA.
[5] Space Telescope European Coordinating Facility.
[6] Osservatorio Astronomico di Padova, Vicolo Osservatorio, 5, I-35122 Padova, Italy.
[7] Royal Greenwich Observatory, Madingley Road, Cambridge CB3 0EZ, United Kingdom.
[8] European Southern Observatory, Karl Schwarzschild Strasse 2, D-8046 Garching, Federal Republic of Germany.
[9] Laboratoire d'Astronomie Spatiale du CNRS, Traverse du Siphon, Les Trois Lucs, F-13012, Marseille, France.
[10] Department of Physics, University College of Cardiff, P.O. Box 713, Cardiff CF1 3TH, Wales, United Kingdom.
[11] Astrophysics Division, Space Science Department of ESA, ESTEC, NL-2200 AG Noordwijk, The Netherlands.
[12] Laboratory for Space Research, Utrecht; postal address: Space Research Institute, Sorbonnelaan 2, NL-3584 CA Utrecht, The Netherlands.
[13] Astronomy Department, University of California, Berkeley, Berkeley, CA 94720.
[14] Institute of Astronomy, Cambridge; postal address: Madingley Road, Cambridge CB3 0HA, United Kingdom.
[15] Max-Planck-Institut für Radioastronomie, Bonn; postal address: Auf dem Hügel 69, D-5300 Bonn 1, Federal Republic of Germany.
[16] Osservatorio Astronomico di Padova.

2. OBSERVATIONS AND DATA REDUCTION

The data presented here were obtained on 1990 August 23 with the FOC in its f/96 mode. The FOC is described in detail in Macchetto et al. (1982) and Paresce (1990). The telescope focus was set at the nominal best focus position, and the spacecraft was pointing in coarse track. For these observing conditions the instrumental point-spread function (PSF) was measured to have a central core of approximately 0".06 radius containing 15% of the energy. The rest of the light is spread out over a region of approximately 2" radius due to the spherical aberration of the primary mirror. The images were taken with the 512×1024 pixel^2 format covering a field of 22×22 arcsec^2 with a pixel size of 48×24 μm corresponding to 0.044×0.022 arcsec^2 on the sky. With this format, the word length is 8 bits allowing up to 256 counts before overflow.

Data taken with two bandpass filters are presented in this *Letter*. The narrow-band interference filter F501N and the medium-band F372M filters were designed to isolate the [O III] 5007 Å and [O II] 3727 Å lines (Paresce 1990). The F501N filter has a peak transmission of 68% at 5010 Å and a FWHM of 74 Å. The corresponding numbers for the F372M filter are 73% at 3700 Å and 412 Å. The complete system was calibrated absolutely using the calibration star BPM 16274 (Turnshek et al. 1990) and found to be within $\pm 20\%$ of the system response tabulated in Paresce (1990). Using these latter values, the sensitivity of the device amounts to 19 and 528 counts s^{-1} for a flat 1 mJy source for the F501N and F372M filters, respectively. The transmission of the F501N filter at the [O III] 5007 Å line is 68%, at the [O III] 4959 Å line 22% and at the Hβ 4861 Å line 0.07%. The transmission of the F372M filter at the [O II] 3727 Å line is 72%, at the [Ne III] 3868 Å line 50%, and at the [Ne III] 3968 Å line 21%.

Three exposures centered on the Mira position were taken with the filters just described: two of a duration of 10 minutes each in the F501N filter and one of a duration of 15 minutes in the F372M filter. At the time of the measurement, the Mira variable had an M7 spectrum and $V = 10.2$ as estimated by Mattei (1990). The raw images were processed as described in Paresce (1990). First, each image was rebinned to a 1024×1024 pixel^2 format and, then, flattened using ground-based flat fields. The flat fields used correct for large-scale variations of instrument response across the field, not the pixel by pixel variations which remain in the processed images. Fixed pattern noise in the camera is not removed.

The frames were then geometrically corrected using an algorithm developed at the STScI that effectively resamples the image with pixels that are equally spaced and have equal areas on the sky. In this way, flux is automatically conserved. Reseau marks were not removed, and no attempt was made to smooth or deconvolve the images since this would introduce errors difficult to quantify at present. The first two F501N images were co-added directly since no registration was necessary. Thus, the final F501N image corresponds to an integration of 20 minutes.

The results of this processing are shown in Figure 1 (Plate L20). The image on the left (Fig. 1, *left*) corresponds to a portion of the 15 minute F372M exposure, while the one on the right (Fig. 1, *right*) corresponds to the same portion of the 20 minute exposure through the F501N filter. Both images are negatives. The orientation on the sky is shown at the bottom right-hand corner where the north direction is inclined 43° to the sample (horizontal) direction. The field of view displayed is 11×5.5 arcsec^2 or one-fourth of the actual image in order better to appreciate the complexity of the northern stream. The distance between successive reseau marks corresponds to 60 pixels or 1".2 in the sky. The gray scale is linear from 0 to 200 counts per pixel. The striped pattern inclined 45° to the horizontal, particularly noticeable in the white saturated areas in the core, is a fixed pattern noise originating in the camera. Assuming R Aqr is at 250 pc (Whitelock 1988), 1" in these images corresponds to a linear scale at the source of 250 AU and a light travel time of 1.4 days.

3. ANALYSIS AND DISCUSSION

The predicted count rates from the core of R Aqr (Mira plus compact wind) are 25 and 108 counts s^{-1} pixel^{-1} in the F501N and F372M filters, respectively. These values greatly exceed the upper limit of the FOC's dynamic range for linear response (Paresce 1990). This explains the inverted appearance of the nucleus of R Aqr in the negative frames shown in Figure 1 in the region where the detector becomes paralyzed near the bottom of the images. The core is surrounded by the aberrated PSF due mainly to the brightest southernmost knot. This cloud of scattered radiation reaches out to a well-defined radius of approximately 2" with the complement of tendrils and rings well established from previous measurements of the instrument PSF with point sources.

Beyond and above this cloud, a number of real features stand out clearly in the images presented here. The shape of the outer edges of the nucleus is preserved by the position of onset of saturation. In the brighter F372M picture on the left, the optical nucleus breaks up into two sources separated by 0".8 $\pm$ 0".1 as determined by the centroid of the dark patches. In the F501N picture that is less saturated, however, the core takes on a complex but well-defined lumpy appearance still dominated by the same two knots that are now seen to be elongated in the PA = 50° direction, approximately. Judging from the position of the centroid of the unsaturated PSF, the brightest spot in this image coincides with the center of the round patch at the southernmost end of the core. This position, most likely, represents that of the Mira itself since it is expected to contribute the bulk of the photons seen there and in the aberrated PSF surrounding it. A small detached knot appears just to the north of the narrow bridge separating the two sources.

Another remarkable feature of the nucleus in the F501N image is the sharp northern edge of the fainter of the two knots running in an almost EW direction. A bright, continuous filament emerges from the tip of this knot. It can be traced all the way up to an opaque object located at 3".6 to the NE of the Mira variable around which it seems to split into two parts. The eastern part falls back onto itself while the western part curls into a prominent loop and, then, continues up until it breaks up into wisps and knots deviating toward the north. All the brighter features in the image are embedded in a faint, tenuous nebulosity of 3"–4" thickness resembling smoke from a chimney. A horizontal cut through the chimney at the height of the opaque obstacle is shown in Figure 2 in counts pixel^{-1} as a function of the sample pixel number. The surface brightness in the [O III] line corresponding to 100 counts pixel^{-1} in this figure is equivalent to 10^{-12} ergs cm^{-2} s^{-1} arcsec^{-2}. One hundred pixels is 2".2 on the sky. It is important to note here that the peak count rates obtained near the obstacle are close to the maximum of the dynamic range of the FOC, and the response, therefore, is expected to be midly nonlinear. We estimate that this effect introduces an uncertainty of $\pm 50\%$ on

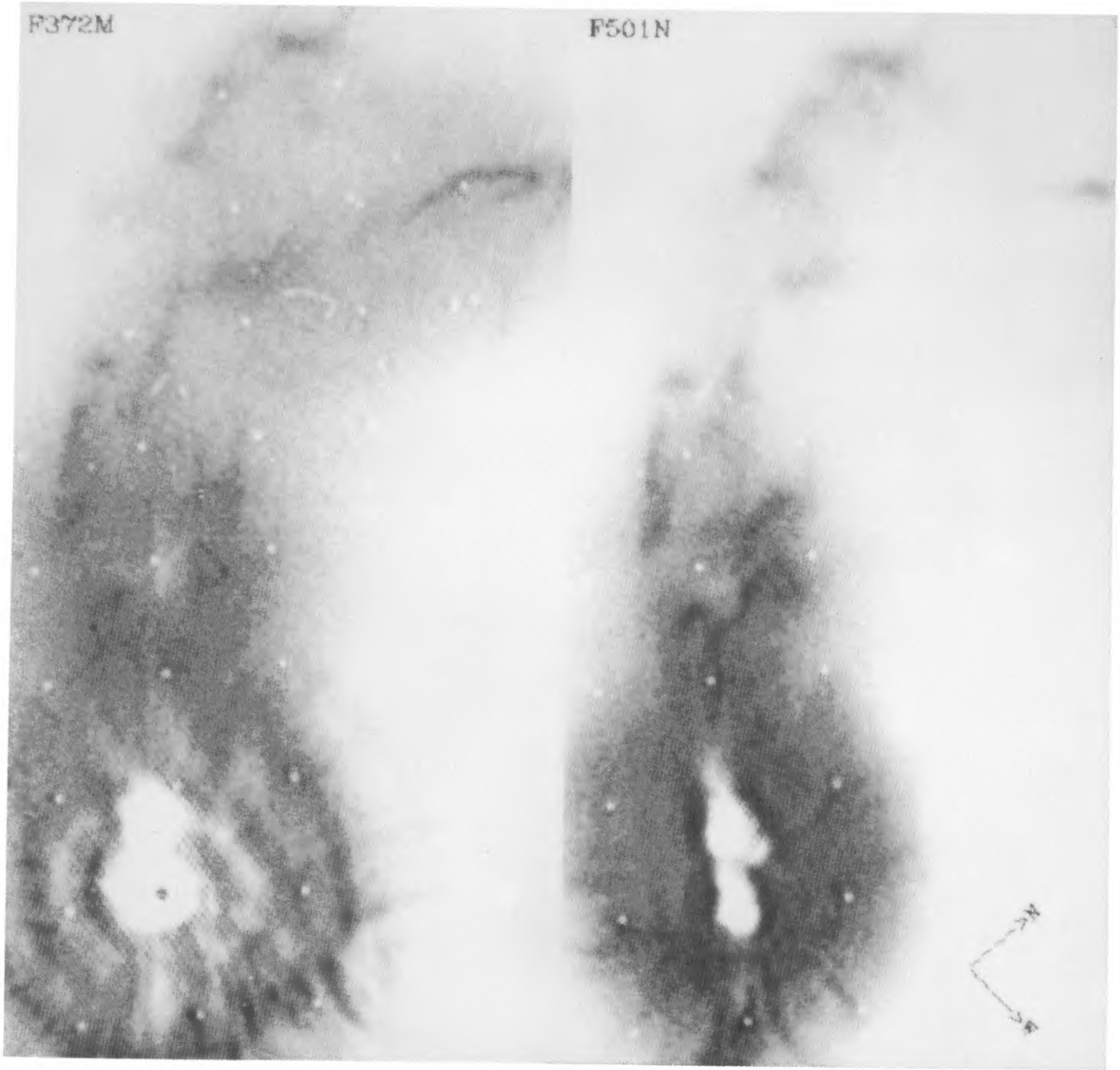

FIG. 1.—*Left panel*: Rebinned, flattened, and geometrically corrected negative image of the core of R Aquarii taken with the FOC through the F372M filter on 1990 August 18. The exposure time is 15 minutes, and the field covered by the image is 11″ in the vertical by 5″.5 in the horizontal direction. The distance between reseau marks is 1″.2. The central bright area is inverted due to saturation of the camera. *Right panel*: Same as left panel except for the filter F501N and an exposure time of 20 minutes.

PARESCE et al. (see 369, L68)

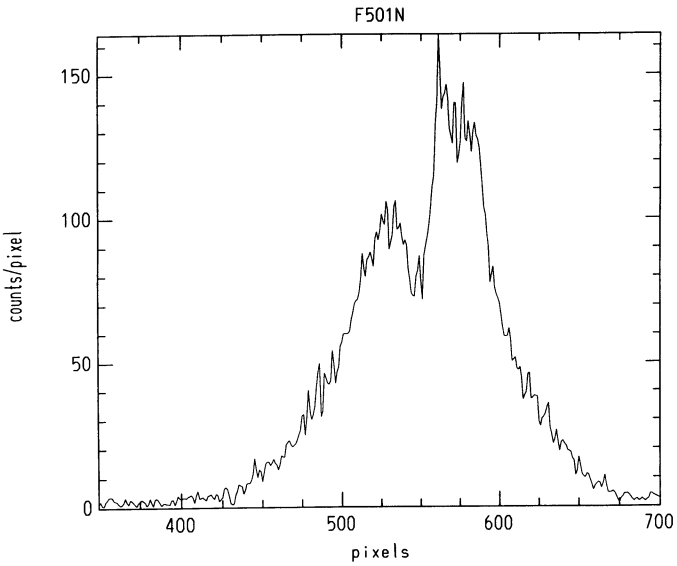

FIG. 2.—Observed counts pixel^{-1} in the F501N image shown in Fig. 1 (*right*) as a function of sample pixel number along the horizontal direction at the height of the loop and dark spot at 3".6 from the center of the lower nuclear knot. Assuming a linear response, the 100 counts pixel^{-1} level corresponds to a surface brightness of 10^{-22} ergs cm^{-2} s^{-1} arcsec^{-1}. The loop is the brightest feature at 150 counts pixel^{-1} just to the right of the dark spot.

absolute intensities in this region. Intensities of the weaker features to the NE are of order one-half to one-third of those near the loop and should be accurate to $\pm 20\%$.

The F372M image on Figure 1 (*left*) shows similar structure in general but with some notable differences. Here, the most prominent filament is the eastern one which stretches in an almost unbroken arc across the frame to the north. The opaque area is still visible, but the loop and geyser-like filament are not easily recognizable in this bandpass probably because of saturation effects. The diffuse nebulosity is even more prominent and extended than in the [O III] line. While the NE stream of material is very obvious, there is definitely a much fainter counterstream extending to the SW of the nucleus. It is noticeable at the very bottom of Figures 1 (*left*) and 1 (*right*), but it extends only a few arcseconds from the Mira variable position. In the extended 22 × 22 arcsec^2 image, very faint nebulosity appears at the SW edge of the frame in the form of a knot and a curved filament emanating from it. These features appear brightest in the F372M filter. Ground-based high-resolution optical and radio images of R Aqr are consistent with the overall, large-scale structure observed with *HST* and described above. Specifically, feature A in the 2 cm radio maps of Kafatos et al. (1989) falls right on the loop to the NW of the opaque obstacle, while the correspondence in both position and shape between the two knots in the nucleus seen in Figure 1 (*right*) and features C1 and C2 is striking. The area around features B and D described in detail by Paresce et al. (1988) is seen to be resolved in a number of knots, wisps, and filaments residing at the top of Figures 1 (*left*) and 1 (*right*) and curving to the north. The *HST* images provide, with their much higher spatial resolution in the optical, a much more detailed picture of the nebula than was possible from the ground.

With these images and the absolute calibration given in § 2, we can derive a lower limit to the [O III]/[O II] line intensity ratio anywhere in the field except in the saturated core where the actual signal level is unknown. This ratio is a powerful diagnostic of the ionization structure of the emitting gas and, therefore, of the principal emission mechanism of the nebula. Contamination from Hβ emission in the F501N bandpass is negligible, but the wider F372M bandpass allows the possibility of contributions to the observed signal from other lines besides the [O II] 3727 Å line, especially the [Ne III] lines at 3868 and 3968 Å. Not knowing, *a priori*, the latter line strengths, even though they are expected to be weaker than the [O II] line in the nebula from ground-based low spatial resolution observations (Wallerstein & Greenstein 1980; Hollis, Wagner, & Oliversen 1990), the derived [O III]/[O II] line ratio should be considered a lower limit. We find that this ratio is greater than 1 in all the prominent filaments to the NE of the nucleus. It reaches a high of 2.7 along the uppermost arc of nebulosity in the images presented here and 3.2 in the loop to the NW of the obstacle at 3".6 of the Mira variable position. We expect that the main source of error in the determination of this line ratio is the nonlinearity of response of the instrument discussed in the preceding paragraphs. We are in the process of gathering the data necessary to more accurately characterize the in-orbit behavior of the FOC in this regard in order to refine the error analysis for a future publication, but we do not expect our main conclusion reported here to be affected. We also note for completeness that the derived values of this ratio must be insensitive to any deconvolution scheme adopted in the future since the PSFs measured through the two filters with calibration stars are identical to within $\pm 10\%$ or less.

Comparison with theoretical calculation shows that, if the ionization structure of the gas is radiation-bounded, this ratio should be significantly less than 1 for a stellar-type photoionization source (Veilleux & Osterbrock 1987; Baldwin, Phillips, & Terlevich 1981). The observed ratios can be explained, in this case, only with a power-law ionizing radiation source as might be expected from synchrotron emission, for example. This result would also be consistent with recent determinations of optical line ratios from the ground (Burgarella & Paresce 1991) and the nonthermal nature of part of the core (Kafatos et al. 1989). A shock-heating emission mechanism might be difficult to support with the observed ratios, although the observed morphology of the inner nebula, the presence of the SiO maser, the high [O III]/Hβ ratio, and the kinematic structure all point to such an interpretation. It is quite possible, on the other hand, that the ionization structure in the nebula is density-bounded due to the relatively small densities there ($n_e = 10^4$ cm^{-3}, typically). In this case, one can imagine gas distributions such that the [O III]/[O II] ratio is significantly higher than 1 even with a stellar ionization source.

The continuous, unbroken morphology of the prominent filament extending from the nucleus to at least 4" or 1000 AU to the NE indicates that the ejection of material is also continuous, not the sporadic phenomenon suggested by Kafatos, Michalitsianos, & Hollis (1986). Clearly, more observations with the full complement of *HST* instrumentation including the spectrographs will be required to make more progress in our understanding of the physical mechanisms powering this fascinating object. The observations presented here also show clearly that the core of R Aquarii is very complex with structure down to the resolution limit of *HST* and that, therefore, one should exercise some caution in interpretation of normally unresolved features on the ground. Moreover, the well-known temporal variations on relatively short time scales argue for frequent observations to monitor the evolution in time of the observed inner structures.

The Faint Object Camera is the result of many years of hard work and important contributions by a number of highly dedicated individuals. In particular, we wish to thank ESA *HST* Project Manager Robin Laurance, the ESA/*HST* Project Team, and the European contractors for building an outstanding scientific instrument. The FOC IDT Support Team, D. Baxter, P. Greenfield, R. Jedrzejewski, and W. B. Sparks, acknowledge support from ESA through contract 6500/85/NL/SK. P. Crane and I. R. King acknowledge support from NASA through contracts NAS5-27760 and NAS5-28086. This *Letter* has also benefited greatly by the assistance of Denis Burgarella and illuminating discussions with Manfred Vogel.

REFERENCES

Baldwin, J. A., Phillips, M. M., & Terlevich, R. 1981, PASP, 93, 5
Burgarella, D., & Paresce, F. 1991, ApJ, in press
Hollis, J. M., Wagner, R. M., & Oliversen, R. J. 1990, ApJ, 351, L17
Kafatos, M., Hollis, J. M., Yusef-Zadeh, F., Michalitsianos, A. G., & Elitzur, M. 1989, ApJ, 346, 991
Kafatos, M., Michalitsianos, A. G., & Hollis, J. M. 1986, ApJS, 62, 853
Kenyon, S. J. 1986, The Symbiotic Stars (Cambridge: Cambridge University Press)
Macchetto, F., et al. 1982, in The Space Telescope Observatory, ed. D. N. B. Hall (NASA CP-2244), 40
Mattei, J. A. 1990, AAVSO observations, private communication
Mattei, J. A., & Allen, J. 1979, JRASC, 73, 173
Merrill, P. W. 1950, ApJ, 112, 514
Michalitsianos, A. G., & Kafatos, M. 1988, in The Symbiotic Phenomena, ed. J. Mikolajewska, M. Friedjung, S. J. Kenyon, & R. Viotti (Dordrecht: Reidel), 235
Paresce, F. 1990, The Faint Object Camera Instrument Handbook, Version 2.0 (Baltimore: Space Telescope Science Institute)
Paresce, F., Burrows, C., & Horne, K. 1988, ApJ, 329, 318
Schulte-Ladbeck, R. E. 1988, in Polarized Radiation of Circumstellar Origin, ed. G. V. Coyne, et al. (Vatican City: Vatican Observatory), 319
Solf, J., & Ulrich, H. 1985, A&A, 148, 274
Turnshek, D. A., Bohlin, R. C., Williamson, R. L., Lupie, O. L., Koornneef, K., & Morgan, D. H. 1990, AJ, 99, 1243
Veilleux, S., & Osterbrock, D. E. 1987, ApJS, 63, 295
Wallerstein, G., & Greenstein, J. L. 1980, PASP, 92, 275
Whitelock, P. A. 1987, PASP, 99, 573
———. 1988, in The Symbiotic Phenomena, ed. J. Mikolajewska, M. Friedjung, S. J. Kenyon, & R. Viotti (Dordrecht: Reidel), 47
Willson, L. A. 1988, in Polarized Radiation of Circumstellar Origin, ed. G. V. Coyne et al. (Vatican City: Vatican Observatory), 447